Electronic Supplementary Information

Thermal Characterization of Carbon Nanotube Foam using MEMS Microhotplates and Thermographic Analysis

*Cinzia Silvestri,[a] Michele Riccio, [b] René H. Poelma,a Bruno Morana,[a] Sten Vollebregt,[a] Fabio Santagata,[a] Andrea Irace,[b] Guo Qi Zhang [a] and Pasqualina M. Sarro [a] **

[a] Department of Microelectronics, Delft University of Technology, Feldmannweg 17, 2628CT Delft, The Netherlands.
* E-mail: P.M.Sarro@tudelft.nl;

[b] Department of Electrical Engineering and Information Technologies, University of Naples Federico II, Via Claudio 21, 80125 Naples, Italy.

S1. CNT Customized Shapes by Lithographic Patterning

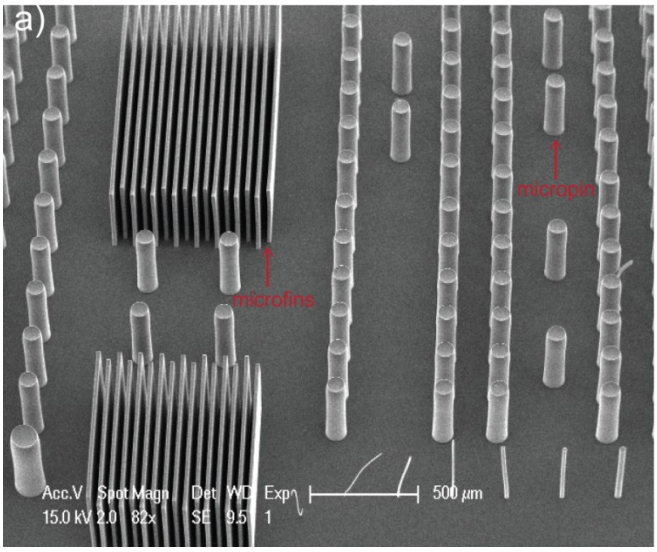

Fig. S1: SEM images customized shape of high-aspect ratio CNT nanofoams defined by photolithographic process.

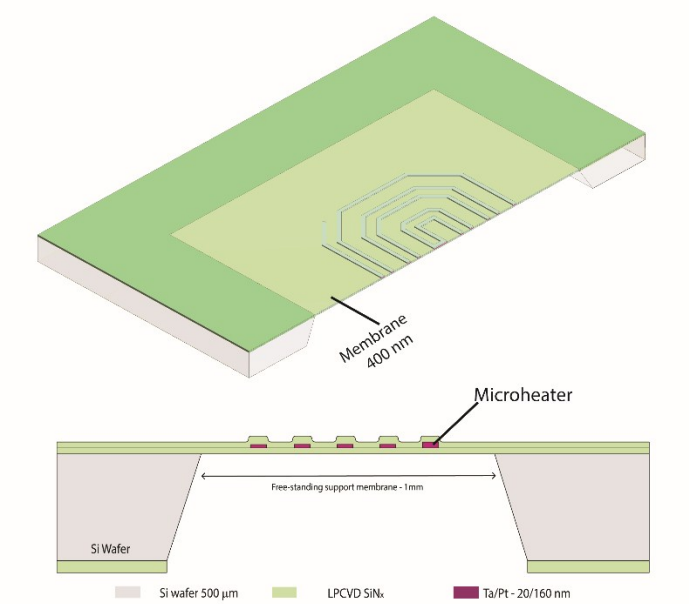

Fig. S2: Three dimensional sketch and cross-section of the microhotplate (MHP) before CNT growth.

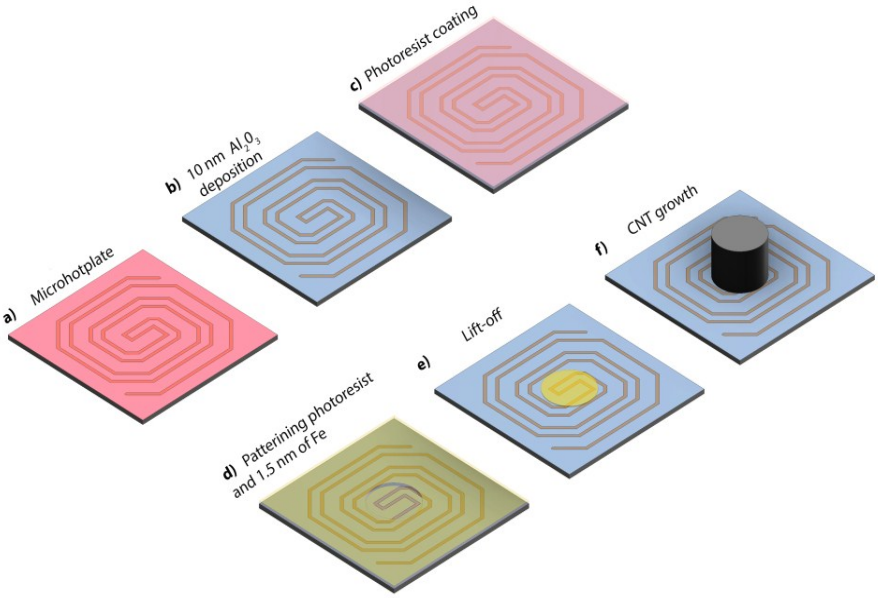

Fig. S3: CNT growth process on MHP. (a) On a bare microhotplate device (b) 10 nm of A_2O_3 barrier layer was sputtered. The wafer was (c) coated with 2 µm of positive resist and patterned. (d) Then 1.5 nm of Fe catalyst was evaporated on the entire surface. (e) Once performed the Lift-off, the stack of all required layer for the CNT growth was ready. Finally, the sample was loaded

on a CVD reactor and (f) the CNTs were grown at 600°C for 5 minutes, to achieve the desired aspect-ratio.

S2. Measurement setup

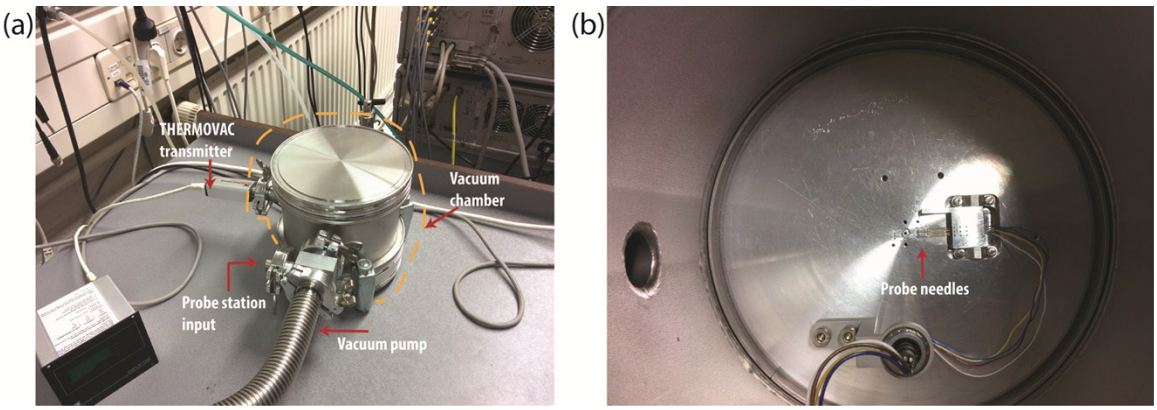

Fig. S4: The electrical characterization is performed loading the MHP in a stainless still vacuum chamber connected to a vacuum pump and a probe station. (a) Chamber connected to the vacuum pump and a THERMOVAC transmitter. (b) Close-up of the interior of the vacuum chamber equipped with four probe needles.

S3. Temperature Recorded by Electrical and High-Resolution Micro-Thermography

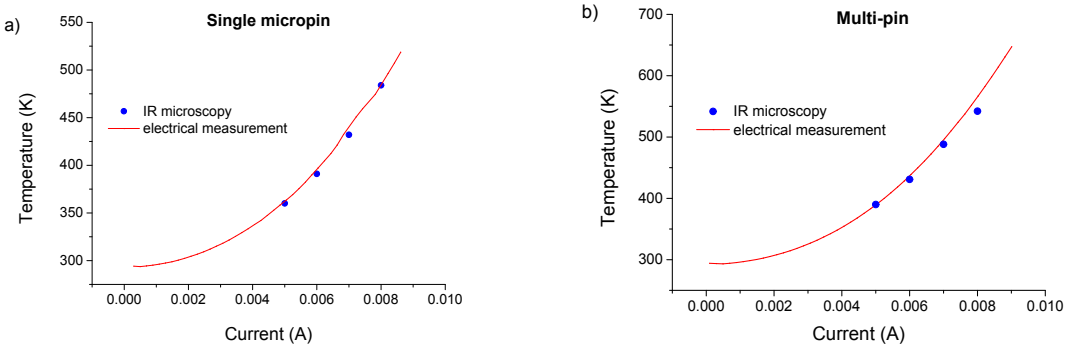

Fig. S5: Comparison between temperatures recorded by electrical measurement and high-resolution micro-thermography for (a) single micropin and (b) multi-pin arrangements.

S4. Relative Power Dissipated through Conduction, Radiation and Convection

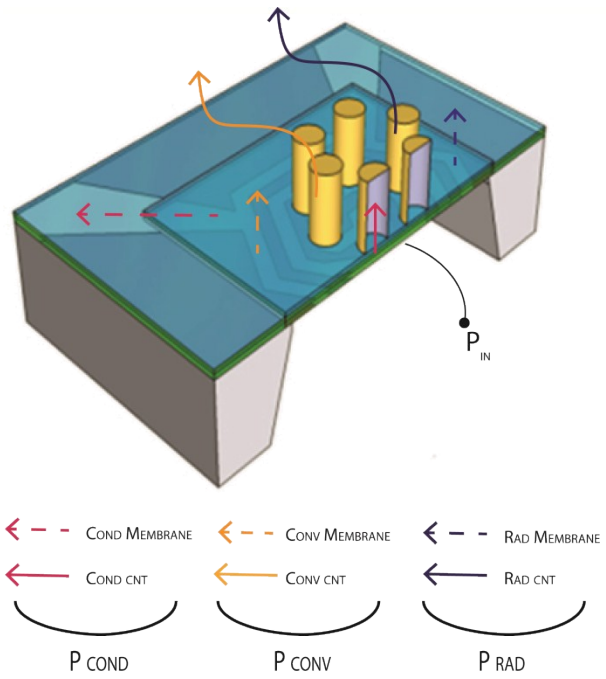

Fig. S6: The heat generated by the microhotplate (P_{IN}) is dissipated by conduction, radiation and convection through the membrane and the micropin configuration. The overall heat transfer contributes are measured in terms of dissipated power (P_{cond}, P_{conv}, P_{rad}).

Table S1: Relative power dissipated by the reference and both CNT nanofoam configurations at T_{max} = 575 K in air. For all the configurations the convective contribution is the most significant. The decrease in the conductive contribute due to the CNT insertions is also visible.

Sample	Power (mW)	Conduction (%)	Radiation (%)	Convection (%)
Reference	21.25	28.1%	1.7%	70.2%
Multi-pin	23.71	21.9 %	2.8 %	75.3 %
Single micropin	27.63	16.4 %	5.8 %	77.8 %

S5. One-Dimensional Heat Transfer Model

The heat transport analysis in micropin is primarily achieved through Fourier`s equation:[1]

$$\frac{d^2T_s}{dx^2} - \frac{H_c P}{k_{eff}A_c}(T_s - T_{surr}) - \frac{\epsilon\sigma P}{A}(T_s^4 - T_{surr}^4) = 0 \quad \text{(S1)}$$

$$\frac{d^2T_s}{dx^2} - \frac{H_{TOT}P}{k_{eff}A_c}(T_s - T_{surr}) = 0 \quad \text{(S2)}$$

where P is the perimeter of the fin cross section ($P = \pi D$), k_{eff} is the effective thermal conductivity of the CNT nanofoam, and A_c is the cross sectional area of the micropin ($A_c = \pi D^2/4$), T_{surr} is the surrounding temperature. By defining $H_{tot} = H_c + H_{rad}$ and $m = \sqrt{H_{TOT}P/k_{eff}A_c}$, the second-order differential equation can be written as:

$$\frac{d^2T_s}{dx^2} - m^2(T - T_{surr}) = 0 \quad \text{(S3)}$$

The *first boundary condition* (**BC 1**) regards the micropin base temperature, T_b.

$$T_s|_{x=0} = T_b \quad \text{(S4)}$$

The *second boundary condition* (**BC 2**) assumes an adiabatic tip, with a corrected micropin length, $L_c = L + D/4$, that takes into account the convective and radiative effects at the micropin tip.

$$\left.\frac{dT_s}{dx}\right|_{x=Lc} = 0 \quad \text{(S5)}$$

The resulting temperature distribution along x of the micropin is:

$$T_s(x) = T_{surr} + \frac{\cosh m(L_c - x)}{\cosh mL_c} * (T_b - T_{surr}) \quad \text{(S6)}$$

Both T_b and T_{tip} can be extracted from the high-resolution IR thermal maps taken at different power regime.

By evaluating the temperature distribution at the fin tip, $T_s|_{x=L_c} = T_{tip}$, m and consequently k_{eff} can be determined as following:

$$m = \frac{1}{L_c} arcosh\left(\frac{T_b - T_{surr}}{T_{tip} - T_{surr}}\right) \tag{S7}$$

$$k_{eff} = \frac{4\,H_{TOT}}{m^2\,D} \tag{S8}$$

H_{TOT} is evaluated between the fin wall average temperature and the ambient, at $T_{ref} = (T_{s\_avg} + T_{surr})/2$, where $T_{s\_avg} = (T_b + T_{tip})/2$.

S6. Raman Spectroscopy

To determine the quality of the CNT nanofoam we performed a Raman characterization using an Horiba LabRAM HR Raman spectroscope. The excitation wavelength of the laser source was 488 nm with a power below 1 mW to not burn the sample. The first-order band and the deconvoluted spectra are shown in Figure S6. The D peak is located around 1350 cm^{-1} and represents the CNT defects, as carbonaceous impurities or broken sp^2 bond. The G peak near 1580 cm^{-1} depends on the graphitic nature of the nanofoam. The quality is widely assessed by intensity ratio I_D/I_G.[2]

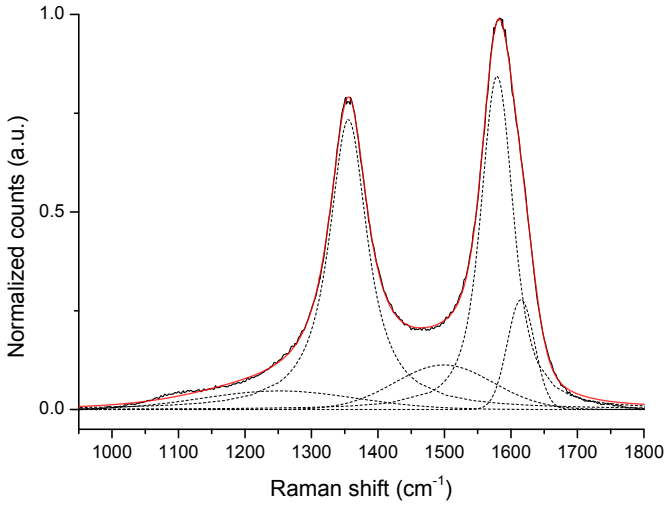

Fig. S7: First-order band of the as-grown CNT nanofoam, normalized to the G peak. It shows an I_D/I_G equal to 0.93.

S7. Overlapping between Neighbouring CNTs

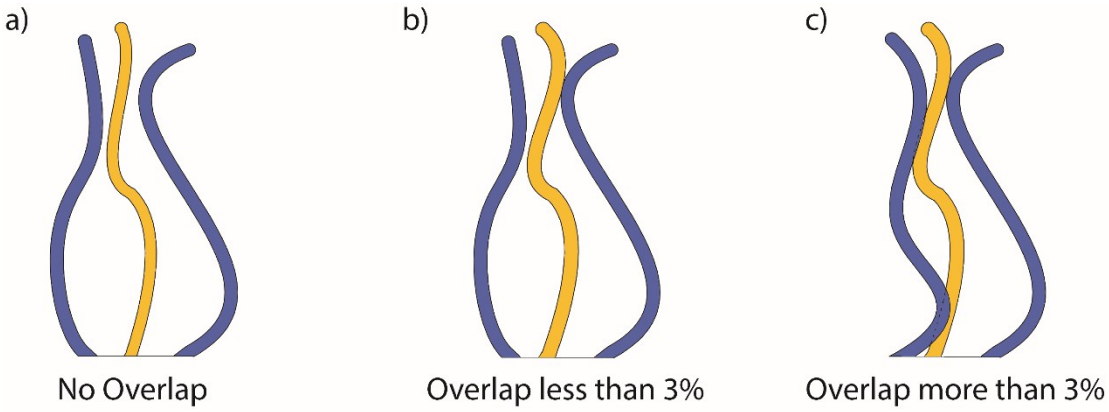

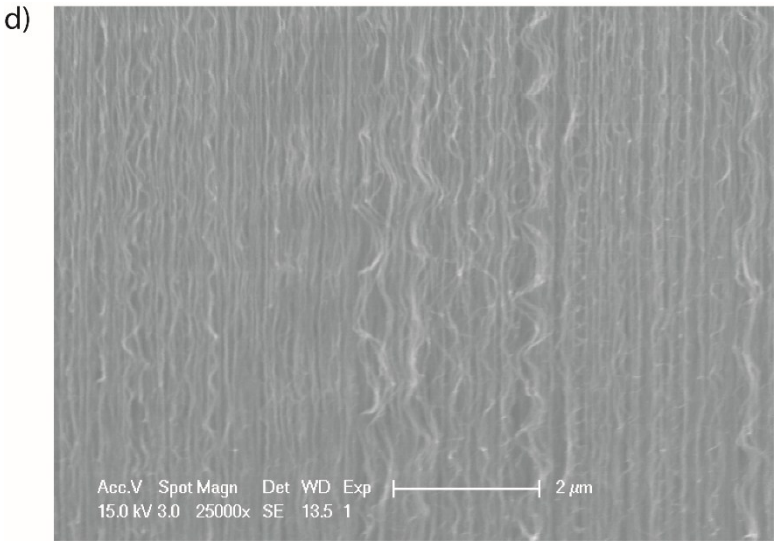

Fig. S8: Schematic illustration regarding the maximum overlapping length of CNTs before their thermal performance degradation.[3] (a) No overlap among neighboring CNTs; (b) Overlap less than 3% (CNT in the center); (c) Overlap more than 3% of the total CNT length. (d) SEM image showing the periodic waviness of the vertically aligned CNT nanofoam grown on top of the MHP. The rough estimated overlapping, made visual inspection, goes 4% to 22% depending from the location.

Reference

1 T. L. Bergman, F. P. Incropera and A. S. Lavine, *Fundamentals of Heat and Mass Transfer*, 2011.

2 Y. Ouyang, L. M. Cong, L. Chen, Q. X. Liu, Y. Fang, *Phys. E Low-dimensional Syst. Nanostructures* 2008, ***40***, 2386-2389.

3 A. E. Aliev, M. H. Lima, E. M. Silverman and R. H. Baughman, *Nanotechnology*, 2010, **21**, 035709.